CHARACTERIZATION OF LUNAR CRUST MINERALOGY WITH M³ DATA. Y. Sun[1] and L. Li[1], [1]Indiana University- Purdue University at Indianapolis, Indiana, USA (yingsun@iupui.edu).

Introduction: Analysis of the lunar samples returned by the Apollo and Luna missions (1969-1976) indicates the presence of compositional heterogeneity in the lunar crust [1]. However, the exact details of lunar crustal structure and evolution remain contentious because of the limited representativity of the returned lunar samples. Recently aquired global, high-spatial resolution hyperspectral Moon Mineralogy Mapper (M³) images provide a new opportunity to examine compositional trends across the entire Moon. Using M³ images, a systematic screening of lunar crater central peaks was conducted to investigate the mineral composition of the lunar crust with the ultimate goal of addressing its evolution.

In this study, 166 lunar craters were selected from 1559 lunar craters listed in the USGS crater database. This selection is based on crater diameter, DEM data and M³ data availability in order to assure that the examined craters have the undisturbed central peaks and expose deep pristine materials from the lunar crust or upper mantle. The selected craters (Fig. 1) are ~35.1 km to ~199.5 km in diameter (d), and have excavation depth (D) ranging from ~5.05 km to ~33.21 km based on $D=0.109*d^{1.08}$[2].

Dataset and Method: M³ L2 images of 166 craters were downloaded from the NASA PDS website. These images at a spatial resolution of 140 m and spectral resolutions of 20-40 nm were geometrically corrected and smoothed for noise reduction. For the geometric correction, the original reflectance images were warped based on latitude and longitude values of each pixel. For the noise reduction, pixels with negative reflectance values or within shadow were eliminated, and the spectra were smoothed using a moving window average method. After spectral smoothing, 72 bands in the spectral range 540-2537 nm were retained for further analysis.
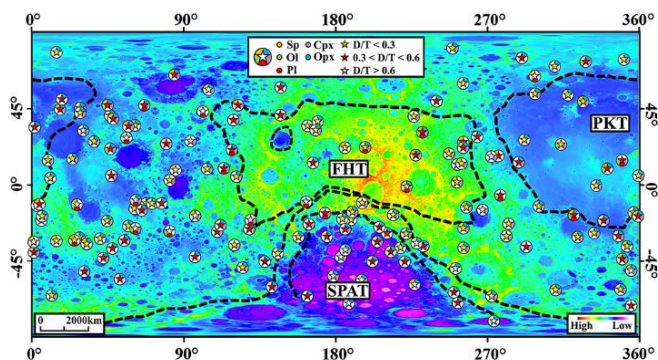

Fig. 1 Location of examined central peaks overlaid on a LOLA DEM of the Moon. Solid stars represent relative depth (D/T) and filling fringe colors show identified minerals in this study. Black dash lines describe three distinct lunar terranes.

Continuum removal was applied to each image spectrum to isolate mineral diagnostic absorption features from the spectral continuum. Based on the diagnostic absorption feature of common lunar minerals (Mg-spinel [Sp] ~ 2 µm, Olivine [Ol] ~ 1.05 µm, Crystalline plagioclase [Pl] ~ 1.25 µm, Orthopyroxene [Opx] < 0.95 µm, ~2 µm, Clinopyroxene [Cpx] > 0.95 µm, ~ 2 µm), we created a set of criteria for determining the presence of these minerals. The presence of each mineral was identified with absorption depth of 0.05 as a lower limit and using 0.02 as upper limit to eliminate other minerals. In order to reduce the uncertainties induced by the imperfect thermal removal as well as illumination differences due to local topography, multi-temporal M³ images were processed and analyzed for each crater to ensure the reliability of the mineral detection. On the basis of previous mineral spectral mixing experiments [e.g. 5, 6], pyroxene (Py) is a spectrally dominating mineral in mineral mixtures and delectable even at 10%, but other minerals must have relatively high abundance to be detectable. Therefore, the pixels showing debatable minerals are expected to be relatively pure except those for pyroxene (Py). A quantitative analysis was conducted to assess the likelihood for the presence of each mineral in the investigated central peaks. The minimum number of pixels (NP) was used for Sp, Ol and Pl, and the number of craters (NC) for Py. Note that the minimum NP is a conservative and relative estimate for the presence of minerals considering detection inconsistency among multi-temporal images. While NC can be used to compare the importance of Cpx relative to Opx, it is not applicable for comparison between Py and other minerals.

The ratio of excavation depth (D) to crustal thickness (T) was used to describe the vertical variation of mineralogy in the lunar crust. Based on the crustal thickness (T) derived from Gravity Recovery and Interior Laboratory (GRAIL), all the investigated crater central peaks were determined to originate from lunar crust except for Petavius and Humboldt.

Results and Discussion: Among the 166 investigated craters, 41 of them are Sp-bearing [7], 15 Ol-bearing [8], 20 Pl-bearing and 151 Py-bearing (Fig. 1). This compositional variability is first compared among different terranes without considering the origin depth of the peaks. As shown in Fig. 2A, PKT shows higher likelihood for the presence of each mineral considered here than both FHT and SPAT; FHT has higher likelihood in the presence of Ol, Pl and Cpx than SPAT, but the likelihood for Opx is the same for FHT and SPAT. The high likelihood of PKT

for the presence of mafic minerals was also shown in the global iron map of [9]. More Cpx-bearing central peaks are determined in FHT than SPAT, implying the FHT is Ca-rich as compared with SPAT. It is worth to note that in SPAT, no Ol-bearing central peaks were identified; more Opx were detected than Cpx, indicating that the major composition of the upper mantle might be Opx instead of Ol. This is in agreement with results from cratering simulation [10] and seismic studies of the lunar upper mantle [11].

When the origin depth of crater central peak is factored into the analysis of mineral composition in the lunar crust, the global investigation reported here suggests a 'new' three-layer model (Fig. 2B, Fig. 3). The uppermost layer (D/T<0.3) within a depth range less than 10 km, mainly consists of ferroan anorthosite and Mg-spinel anorthosite in addition to norite and gabbro. PKT has the highest likelihood for the presence for Sp, Ol and Py. FHT contains Pl, Sp, Py and sparse Ol (NP=0.25%). In SPAT, only Py and sparse Sp could exist. While the content of Py is shown to be higher, the crater peaks showing the detected Py most likely represents the mixture of a large proportion of plagioclase and a small proportion of Py because the way for assessing Py differs from that for other minerals.

The middle layer (0.3<D/T<0.6) ranging from ~10 to ~20 km, is rich in most of the common minerals except Pl. Within this layer, PKT exhibits high likelihood for the presence of mafic materials and Sp. In contrast, FHT and SPAT show a lower possibility of the presence for all the minerals than PKT. In particular, SPAT doesn't show the presence of Ol and Sp. Pl is equally detected in all three terranes within this depth range, but the likelihood of the presence is relatively low compared to the deeper layer. These observations indicate that the post-magma ocean magmatisms were more frequent within in the middle layer of the PKT lunar crust, which is consistent with the observations made for lunar thorium [12].

The lowermost layer (D/T>0.6) including lower crust and a part of crust-mantle interface, has been detected to have the largest amount of Pl (nearly pure ferroan anorthosite). Pl has been identified in both FHT and PKT but not in SPA. The SPA basin was confirmed to excavate the lunar upper mantle [10] and most of the lunar crust in SPA may be removed in the basin formation process, thus the observation to SPA may represent the compositions of the upper mantle rather than the lower crust. Based on our observation, we could speculate a global anorthositic layer exist in the lowermost crust. This layer may retain the original crustal composition produced by the Lunar Magma Ocean. In contrast, the middle and uppermost layers have been heavily modified by secondary magmatisms and impact cratering.

Consdiering the mineral variation within the entire lunar crust, Pl increases with depth and Ol and Sp are clustered in the middle layer. Py decreases with depth in PKT; Cpx decreases with depth in FHT, but is more abundant in the middle layer of SPAT; more Opx is detected in the middle layer than the other two layes for FHT and SPAT. These results lead to the following conclusions. First, a global pristine anorthositic layer may exist in the lower crust. Second, most of the secondary magmatisms should occur in the middle crustal layer underneath PKT. While Py also shows a compositional trend with depth, the variation could be an artifact due to the variation of crater population with depth. This should be taken into account in the future study. To validate this 'new' three-layer model, additional regions (e.g. basins, crater wall and ejecta) and datasets (e.g. LRO, Diviner) need to be analyzed.

References: [1] Heiken G. et al. (1991) *Lunar Sourcebook, Cambridge Press*. [2] Cintala M. J. and R. Grieve (1998) *Meteoritics & Planet. Sci.*, 33, 889-912. [3] Clark R. N. et al. (2011) *JGR*, 116(E6). [4] Besse S. et al. (2013) *Icarus*, 222(1), 229-242. [5] Crown, D. A. and Pieters C. M. (1987) *Icarus* 72, 492-506. [6] Cloutis E. A. et al. (1986) *JGR*, 91, 641-653. [7] Sun Y. et al. (2013) *LPS XLIV*, Abstract #1393. [8] Sun Y. and Li L. (2014) *LPS XLV*, Abstract #1653. [9] Lucey P. et al. (1995) *Science* 268, 1150. [10] Melosh H. J. et al. (2014) *LPS XLV*, Abstract #2505. [11] Khan, A., et al. (2006) *JGR*, 111(E5). [12] Warren P. H. et al. (2001) *GRL*, 28(13) 2565-2568.
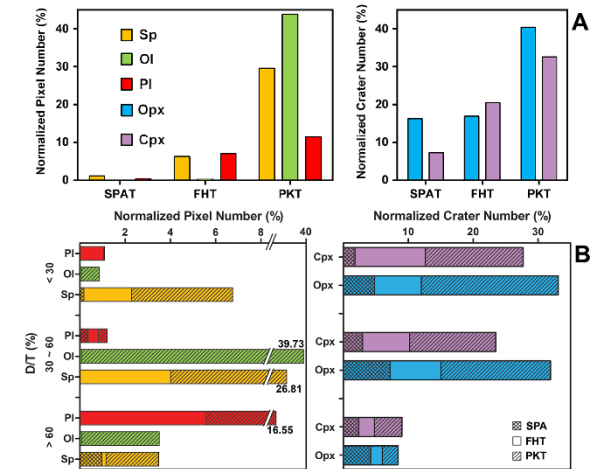

Fig. 2 The likelihood for the presence of identified minerals in three terranes with respect to horizontal (A) and vertical (B) dimension of the lunar crust. $NP_{Sp}+NP_{Ol}+NP_{Pl}=1$ for detected Sp, Ol and Pl and $NC_{Cpx}+NC_{Opx}=1$ for detected Cpx and Opx. The relative depth measured by D/T of central peaks is shown in the vertical axis.
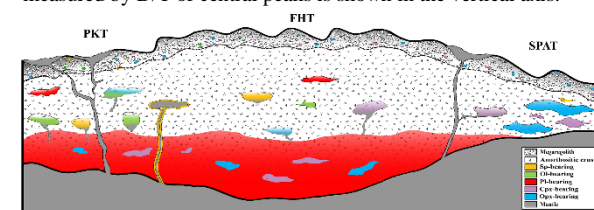

Fig. 3 Schematic cross section of the lunar crust